

# Ab Initio Molecular Dynamics Simulations of (101) Surfaces of Potassium Dihydrogenphosphate

Damien J. Carter<sup>†,‡</sup> and Andrew L. Rohl<sup>†,‡,\*</sup>

<sup>†</sup>Nanochemistry Research Institute, Department of Chemistry, Curtin University of Technology, GPO Box U1987, Perth, WA, Australia, 6845

<sup>‡</sup>iVEC, “The Hub of Advanced Computing in Western Australia”, Technology Park, Kensington, WA, Australia

**ABSTRACT:** We present an *ab initio* molecular dynamics study of bare and hydrated (101) surfaces of KDP. We examine the dynamical nature of the hydrogen bonding in the high and low temperature phases of bulk KDP and find evidence to support the theory that hydrogen atoms oscillate between two off-center positions in the high-temperature phase. We report the translational relaxation of the surface species on the (101) surface and find good agreement with experimental results, particularly with reference to the direction of the relaxation. We find a strongly hydrogen bound water layer close to the KDP surface, comparing closely to a highly ordered water layer observed experimentally. Overall, there is good agreement with the results of nanoscale experimental studies, demonstrating the effectiveness of *ab initio* molecular dynamics calculations at simulating bulk and surface properties.

## INTRODUCTION

Potassium dihydrogenphosphate (KDP) is one of the first materials to be used and exploited for its nonlinear optical properties.<sup>1</sup> At room temperature, KDP forms a paraelectric phase in the tetragonal  $I4_2d$  space group.<sup>2</sup> KDP undergoes a phase transition at 122 K<sup>3</sup> to a ferroelectric phase in the orthorhombic  $C_{2v}$  1-setting space group, as described by Baur.<sup>4</sup> The structure of KDP and its phase change from a ferroelectric to a paraelectric material has been the subject of numerous diffraction and scattering studies, as reviewed elsewhere.<sup>2,5</sup> Surface X-ray diffraction (SXRD) studies have examined the relaxation of atoms on the (101) surfaces of KDP.<sup>6–8</sup> The surface structure under aqueous conditions suggests that there are several “ice-like” ordered water layers on the surface.<sup>8</sup> The ice-like phenomena of water adsorption on surfaces has been reported in a wide range of mineral systems, such as mica.<sup>9,10</sup> In recent years, Vlieg and co-workers<sup>11–13</sup> have further examined the (101) and (100) surfaces of KDP with SXRD to determine the affect of pH on the surface structure and relaxations. They find the (100) surface is insensitive to pH, but the (101) surface is pH dependent, with a competition between  $K^+$  and  $H_3O^+$ .

On-going advances in parallel efficiency and linear scaling algorithms now make it possible to simulate larger and more complex systems using quantum mechanics. There have only been a limited number of quantum mechanical studies of bulk KDP.<sup>1,14–18</sup> A number of these studies have examined the nature of the ferroelectric–paraelectric phase transition and attribute the ferroelectricity of KDP as predominantly a redistribution of charge density caused by a change of the P–O distance and a coupled P–O motion, and also a coordinated motion of the heavier P and K atoms. There are very few theoretical studies of the surfaces of KDP. Stack et al.<sup>19</sup> have used DFT to study the (100) surface of KDP, in particular relating to the adsorbing/detaching of growth units. We have previously published a density functional theory study of (101) surfaces of KDP.<sup>18</sup> In this previous work, we employed static surface calculations of

(101) surfaces under vacuum, nitrogen, and aqueous conditions. In general, we found good agreement with the results from experimental SXRD studies.

There is still a large gap in understanding between our static model used to examine surfaces of KDP and the experimental surface studies. Molecular dynamics provides us with another step of complexity toward a better description of the interactions that determine the surface structure of KDP. In this work, we present an *ab initio* molecular dynamics (MD) study of both the bare and hydrated (101) surfaces of KDP.

## METHODOLOGY

*Ab initio* density functional theory (DFT) calculations were carried out using the SIESTA code.<sup>20</sup> A double- $\zeta$  basis set with polarization functions was used for all atoms except oxygen, which had a triple- $\zeta$  basis set with polarization functions. Core electrons are represented by norm-conserving pseudopotentials,<sup>21</sup> and electron exchange–correlation was treated using the generalized gradient approximation (GGA:PBE<sup>22</sup>). For potassium atoms, we explicitly include the 3p orbital in the valence configuration of the pseudopotential. Hartree and exchange–correlation energies were evaluated on a uniform real space grid of points with a defined maximum kinetic energy of 200 Ry. The numerical atomic orbitals were confined to an extent that induces an energy shift in each orbital of 0.01 Ry.

We used *ab initio* molecular dynamics (MD) calculations to examine both the high and low temperature phases of KDP. We generated a  $2 \times 2 \times 2$  supercell of bulk KDP and used a  $3 \times 3 \times 3$  Monkhorst Pack k-grid for reciprocal space integration. A temperature of 20 K was used to simulate the low temperature ferroelectric phase and 298 K for the high temperature paraelectric phase. Variable cell dynamics were performed with the temperature controlled Nose thermostat, enabling us to optimize

**Received:** December 24, 2010

**Published:** April 29, 2011

Table 1. Calculated Cell Parameters and Bond Lengths, Distances, and Angles for Ferroelectric and Paraelectric KDP

	ferroelectric		paraelectric		ferroelectric		
	MD	Expt.	MD	expt.	static calculations		
	20 K	102 K <sup>a</sup>	298 K	293 K <sup>a</sup>	0 K <sup>b</sup>	0 K <sup>c</sup>	0 K <sup>d</sup>
<i>a</i> (Å)	7.40	7.46	7.43	7.45	7.60	7.52	7.56
<i>b</i> (Å)	7.39	7.40	7.43	7.45	7.58	7.45	7.55
<i>c</i> (Å)	6.85	6.93	6.91	6.97	6.98	7.01	6.93
P–O (Å)	1.60	1.52	1.59	1.54	1.57	1.49	1.56
P–O <sub>H</sub> (Å)	1.65	1.58	1.59	1.54	1.63	1.55	1.63
O <sub>H</sub> –H (Å)	1.11	1.10	1.22	1.07	1.08	1.06	1.07
O <sub>H</sub> ···H (Å)	1.38	1.44	1.22	1.43	1.39	1.42	1.42
O <sub>H</sub> ···O (Å)	2.51	2.49	2.44	2.49	2.48	2.48	2.49
O <sub>H</sub> –P–O <sub>H</sub> (deg)	107.7	106.9	109.5	110.5	106.1	106.5	105.8
O–P–O (deg)	111.8	114.8	109.5	110.5	114.3	114.8	115.7
O <sub>H</sub> –H···O (deg)	178.8	177.6	178.6	177.2	177.1		178.3

<sup>a</sup> Results from Nelmes et al.<sup>2</sup> <sup>b</sup> DFT GGA-PBE results from Koval et al.<sup>14</sup> <sup>c</sup> DFT GGA-PBE results from Zhang et al.<sup>23</sup> <sup>d</sup> DFT GGA-PBE results from Carter et al.<sup>18</sup>

the lattice vectors at internal coordinates of the low and high temperature phases. A step size of  $1 \times 10^{-15}$  s was used for all MD calculations, with each simulation running for approximately 10 000 steps. In all cases, dynamical equilibrium (based on energies and/or volume) appeared to be reached in typically 500–2000 steps. Time-averaged MD structures were generated by averaging the coordinates of each atom over approximately 2000 fs for surface calculations and 5000 fs for bulk calculations.

Using the averaged cell parameters and atomic positions of the high temperature 298 K phase, we then cleaved a (101) surface of KDP. There are two possible ways to cut the (101) surface: one produces a cation ( $K^+$ ) terminated surface, and the other produces a dihydrogenphosphate ( $H_2PO_4^-$ ) terminated surface. From our previous *ab initio* density functional calculations,<sup>18</sup> we have shown that the  $K^+$  terminated surface is significantly more stable than the  $H_2PO_4^-$  surface. Surface X-ray diffraction studies of KDP by de Vries et al.<sup>6,7</sup> have also confirmed this. As a result, we only consider the  $K^+$  terminated (101) surface in our *ab initio* molecular dynamics calculations. Constant temperature (fixed cell) MD calculations were performed on the pure (101) surface with a temperature of 298 K, controlled by the Nose thermostat. The simulation was run for approximately 10 000 steps. Using the relaxed surface, the simulation cell was then filled with water molecules, and the MD calculation was repeated with the simulation running for approximately 10 000 steps.

Note that these calculations are extremely computer intensive, which severely restricts the time frame that can be accessed with *ab initio* molecular dynamics calculations compared to molecular dynamics calculations using interatomic potentials.

## RESULTS AND DISCUSSION

The calculated lattice parameters of KDP at 20 and 298 K are compared to those of the experimentally observed paraelectric and ferroelectric phases, and other theoretical studies in Table 1.

From the results in Table 1, we find the calculated cell parameters of the low temperature ferroelectric phase and the high temperature paraelectric phase compare closely to experimentally reported cell parameters. In both cases, the calculated structures are slightly smaller than experimental results. GGA

functionals of inorganic solids typically lead to an overestimation of cell volumes by a few percent; however, GGA functionals are also known to overestimate the strength of hydrogen bonds in strongly hydrogen-bonded systems.<sup>24</sup> This overestimation of the strength of hydrogen bonds between the  $H_2PO_4^-$  groups leads to a slight contraction in the cells.

There has been debate over the KDP ferroelectric–paraelectric phase transition relating to the ordering of the hydrogen in the high temperature phase. Neutron diffraction studies show that in the paraelectric structure, hydrogen atoms occupy two off-center site positions between the oxygen atoms on neighboring phosphates, with 50% probability.<sup>25</sup> The debate relates to how this 50% occupation occurs. One common theory is that above the phase transition temperature there is a disordered arrangement of  $H_2PO_4^-$  groups, while below there is an ordered arrangement.<sup>2</sup> The other main theory is that the protons oscillate between the two equivalent sites between the oxygen atoms.<sup>26</sup> Recent neutron Compton scattering studies of KDP<sup>27</sup> show clearly that the proton is coherent over both sites in the paraelectric phase, a result that invalidates the commonly accepted disorder–order picture of the transition. Using our molecular dynamics results from the low and high temperature phases, we have investigated the nature of the occupation of hydrogen atoms in the off-center positions. We first examine the time-averaged MD high and low temperature structures and calculate the radial distribution function ( $g(r)$ ) for oxygen to hydrogen distances. This is illustrated in Figure 1.

The low temperature ferroelectric phase (20 K) shows two distinct peaks/regions in Figure 1a. The smaller region from 1.0 to 1.2 Å corresponds to O–H bonds in the KDP, while the 1.3–1.5 Å region corresponds to the hydrogen bond O···H distances. As expected, the two peaks in the time-averaged MD structure are sharper than the peaks for the MD structure over the 5000 fs, due to the dynamical nature of the calculations. The high temperature paraelectric phase (Figure 1b) shows a single broad peak/region from 1.15 to 1.3 Å for the time-averaged MD structure. The MD structure shows a broad hump extending approximately 1.0 to 1.6 Å. There are small crests in this broad hump at approximately 1.1 Å and 1.4 Å, which correspond to typical O–H bond and O–H hydrogen distances. The broad

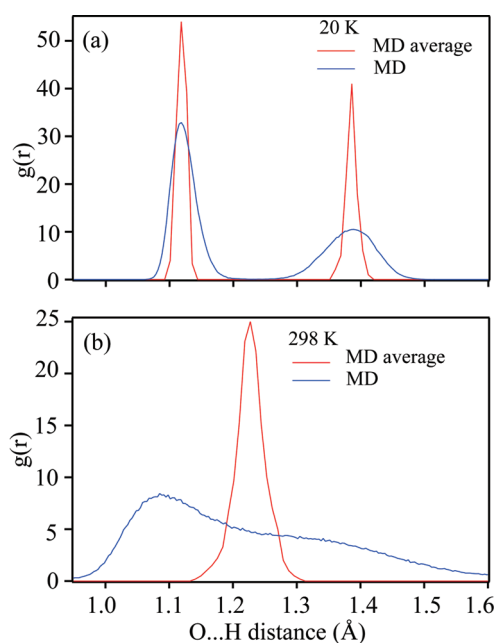


**Figure 1.** Radial distribution function ( $g(r)$ ) of oxygen to hydrogen distances over 5000 fs (MD) and the time-averaged molecular dynamics structure for the (a) low (20 K) and (b) high (298 K) temperature phases of bulk KDP.

hump in the paraelectric phase is caused by the dynamical nature of the simulations, and in particular the oscillation of the hydrogen atom between the two equivalent off-center positions. If there was a simple disorder mechanism in the paraelectric phase, Figure 1b for the MD structure would have shown two distinct peaks (similar to that observed for the ferroelectric phase at 20 K).

The O–H bond length and O···H hydrogen bond distances of 1.22 Å for the 298 K MD structure differ from the experimental structure reported in Table 1. As discussed above, the position of the hydrogen atom is dynamical and typically occupies two off-center positions and can oscillate between them throughout the course of simulation. So to calculate the O–H bond and O···H hydrogen bond distances for the 298 K structure, we use the time-average MD structure (as illustrated in Figure 1b).

To further illustrate the dynamical behavior of the hydrogen atom position, in Figure 2, we illustrate the positions of oxygen and hydrogen atoms along an O···H···O bond/hydrogen bond over a simulation time of 5000 fs, for the 20 and 298 K structures. From Figure 2, one can see that the hydrogen atom in the low temperature (20 K) ferroelectric phase oscillates about its equilibrium off-center position along the O···H···O hydrogen bond, at approximately 1.1 Å from the nearest oxygen atom. The hydrogen atom in the high temperature (298 K) paraelectric phase exhibits much larger oscillations about its equilibrium position. These oscillations correspond to the hydrogen atom oscillating from one equivalent off-center site to the other (i.e., oscillating from  $\text{P}=\text{O}\cdots\text{H}-\text{O}-\text{P}$  to  $\text{P}-\text{O}-\text{H}\cdots\text{O}=\text{P}$ ). If the ferroelectric–paraelectric mechanism was an order–disorder reaction, then the 298 K paraelectric results would have looked very much like the low temperature results with only minimal oscillations around the equilibrium value. The MD results support the theory that hydrogen atoms oscillate between the two off-center positions in the paraelectric phase and are the

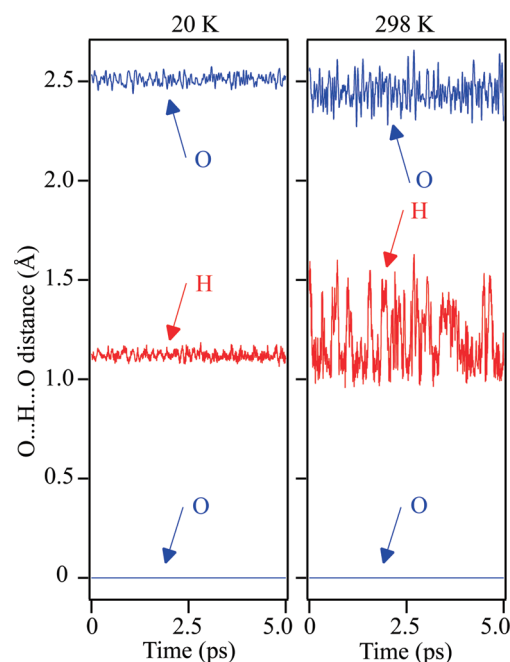


**Figure 2.** Displacement of a hydrogen atom between two oxygen atoms over 5000 fs for the low (20 K) and high (298 K) temperature phases of bulk KDP.

cause of the observed 50% occupation of the off-center positions in this phase.

The paraelectric–ferroelectric transition in KDP is not just related to the hydrogen ordering, but in the low temperature ferroelectric phase, there are also small displacements of potassium and phosphorus atoms along the  $c$  axis. For the KDP bulk at 20 K, the average displacement in the  $c$  direction is 0.04 Å for both the phosphorus and the potassium atoms. Neutron diffraction studies by Nelmes et al.<sup>2</sup> report that the experimental displacements for the low temperature phase of KDP of potassium and phosphorus at 102 K are approximately 0.05 Å. Energy minimization density functional calculations by Zhang et al.<sup>23</sup> report the displacement of phosphorus is 0.06 Å and that of potassium is 0.03 Å. Thus, the calculated displacements of potassium and phosphorus closely match the experimental values from neutron diffraction studies and the calculated values from planewave density functional calculations.

We also examined the electronic structure of the MD averaged paraelectric temperature phase. Examining the band structure, we find an insulator with a band gap of 5.54 eV. Density functional studies of bulk KDP have previously reported band gaps ranging from 4.2 to 6.0 eV.<sup>17,23,28</sup> The band gap of KDP has also been determined experimentally to have values ranging from 7.0–8.8 eV.<sup>29</sup> In general, band gaps calculated using density functional theory are systematically underestimated when compared to experimental values, and this is the case again here.

To quantify the surface relaxations in our simulations of the cation terminated surface, we use the approach taken in the experimental studies of de Vries et al.,<sup>6,7</sup> where a  $\text{H}_2\text{PO}_4^-$  ion is treated essentially as a fixed group, and movements of the central atom in this group (phosphorus) were measured. The displacements of atoms (in the  $z$  direction) are then calculated by comparing the positions in the relaxed and unrelaxed surfaces.

**Table 2.** Translational Relaxations of Species Perpendicular to the (101) Surface of KDP from Static and Molecular Dynamics Calculations

relaxations (Å)	vacuum surface		hydrated surface	
	static <sup>a</sup>	MD	static <sup>a</sup>	MD
$K^+$				
layer 1	−0.25 (−0.29, −0.25)	+0.06 ± 0.05	+0.14 (+0.17, +0.11)	+0.25 ± 0.12
layer 2	−0.01 (−0.02, +0.01)	+0.11 ± 0.05	+0.05 (+0.08, +0.02)	+0.13 ± 0.05
layer 3	0.00 (−0.01, +0.01)	+0.13 ± 0.05	−0.01 (−0.02, 0.00)	+0.13 ± 0.04
layer 4	0.00 (−0.01, +0.01)	+0.00 ± 0.02	0.00 (−0.01, +0.01)	0.00 ± 0.03
$H_2PO_4^-$				
layer 1	+0.12 (+0.18, +0.06)	+0.26 ± 0.10	+0.08 (0.00, +16.00)	+0.24 ± 0.09
layer 2	−0.06 (−0.07, −0.05)	+0.10 ± 0.03	−0.03 (−0.06, 0.00)	+0.18 ± 0.08
layer 3	0.00 (−0.01, +0.01)	0.04 ± 0.03	+0.01 (−0.02, +0.04)	+0.04 ± 0.06
layer 4	0.00 (−0.01, +0.01)	0.00 ± 0.03	0.00 (−0.01, +0.01)	0.00 ± 0.04

<sup>a</sup> Results from Carter et al.<sup>18</sup>**Table 3.** Translational Relaxations of  $K^+$  and  $H_2PO_4^-$  Ions at the (101) Surface of KDP from Theoretical and Experimental Studies

relaxations (Å)	$K^+$	$H_2PO_4^-$
experimental studies		
aqueous solution <sup>a</sup>	+0.10 ± 0.05	+0.04 ± 0.05
static calculations <sup>b</sup>		
0 K vacuum	−0.25 (−0.27, −0.23)	+0.12 (+0.18, +0.06)
0 K hydrated	+0.14 (+0.17, +0.11)	+0.08 (+0.16, +0.00)
molecular dynamics		
298 K vacuum	+0.06 ± 0.05	+0.26 ± 0.10
298 K hydrated	+0.25 ± 0.12	+0.24 ± 0.09

<sup>a</sup> Results from de Vries et al.<sup>6,7</sup> <sup>b</sup> Results from Carter et al.<sup>18</sup>

The 3D periodic simulation cells contain eight layers of  $K^+$  and  $H_2PO_4^-$  ions but have two surfaces (in the  $z$  direction); hence for each species, there are four unique layers (layers 1 and 8 are equivalent, 2 and 7 are equivalent, etc.). The surface relaxations are reported in Table 2 with a negative (−) displacement referring to inward relaxation and a positive (+) displacement referring to an outward relaxation. In Table 2, we compare the layer by layer relaxation for our molecular dynamics calculations versus the results for static surface calculations from our previous study.<sup>18</sup> In Table 2, layer 1 refers to the outermost layer and layer 4 refers to the layer closest to the center of the KDP slab, and error ranges are shown as one standard deviation of the mean value. In experimental SXRD studies, a single site model is used for each surface layer; however, for the static calculations, there are two symmetry-unique positions for each layer, so we report an average relaxation value in Tables 2 and 3 (with the actual values given in parentheses). In the molecular dynamics calculations reported here, there are no longer two symmetry-unique positions for each layer, so we use a single site model for each layer.

One of the most obvious differences in the surface relaxation values for the vacuum surface in Table 2 is the direction of the  $K^+$  species in the outermost layer (layer 1), with static calculations producing a large inward relaxation and MD calculations producing

a small outward relaxation. The (101) surfaces are terminated with  $K^+$  ions, so the outermost  $H_2PO_4^-$  layer (layer 1) is below the surface of the outermost  $K^+$  layer. Under vacuum conditions and at 0 K, the  $K^+$  ions have to contract inward toward the surface. When the temperature is 298 K and the surface is allowed to evolve over time using molecular dynamics, the outermost  $K^+$  layer has a small expansion from its initial configuration. Coupled with this, we also see in MD calculations that there is an outward relaxation of the second and third layers, in contrast to the static calculations where there is negligible change. The relaxations of the  $H_2PO_4^-$  layers for the static and MD calculations are similar in both magnitude and direction.

The layer-by-layer relaxations for the hydrated surfaces in Table 2 show similar trends for the static and MD calculations in terms of the direction of the translational relaxations, although the actual magnitudes do vary. The static calculations of  $K^+$  and  $H_2PO_4^-$  layers only appear to be significant in the outermost layer (layer 1), with the other layers having a negligible change. This was also observed in the vacuum surface calculations. In MD calculations of the hydrated surface, the second  $H_2PO_4^-$  layer and the second and third  $K^+$  layers also show a noticeable relaxation. The static and MD calculations on the hydrated surface both show an outward movement of the outermost (layer 1)  $K^+$  and  $H_2PO_4^-$  layers (see Figure 3 for MD averaged hydrated surface of KDP). The magnitudes of the relaxations of both species in the MD calculations are slightly larger than for static calculations. The static 0 K calculations consisted of 12 explicit water molecules above a surface and a simple geometry minimization to find a minimum energy. In MD calculations, the surface structure and interactions with the water molecules are allowed to time-evolve at a finite temperature, and thus we expect that the magnitudes of the surface relaxations will vary compared to the static calculations. Lateral relaxations of surface atoms in the directions parallel to the surface are approximately 0.04 Å and suggest that there are no large excited surface phonons.

MD simulations enable us to further examine the dynamical behavior of the (101) surface and its interactions with the water molecules. Examining the hydrated surfaces, we find a number of strong hydrogen bonds between the closest water molecules and the (101) surface with typical values of 1.4–1.7 Å. We also examined the position of the hydrogen atoms of surface



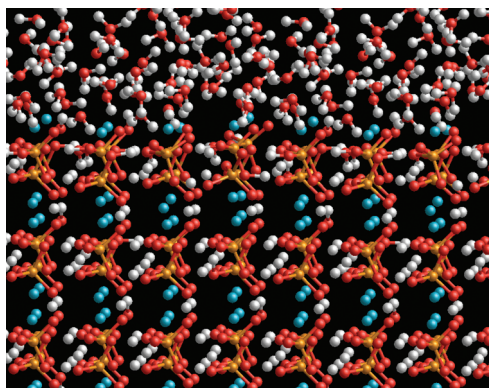


**Figure 3.** MD averaged hydrated surface of KDP. Oxygen, hydrogen, potassium, and phosphorus atoms are represented by red, white, blue, and orange colored spheres, respectively.

$\text{H}_2\text{PO}_4^-$  groups to see if they dissociate into the water molecules or stay in their original positions. Analysis of their locations suggests that the hydrogen atoms of  $\text{H}_2\text{PO}_4^-$  do not exchange with water molecules under the finite temperature dynamics considerations but do form strong hydrogen bonds to the neighboring water layer.

In Table 3, we compare the surface relaxations from our static and MD calculations to the experimental results of de Vries et al.<sup>6,7</sup> The surface relaxations in Table 3 are for the outermost  $\text{K}^+$  and  $\text{H}_2\text{PO}_4^-$  layers. As described above, a negative (−) displacement refers to inward relaxation and a positive (+) displacement refers to an outward relaxation. Error ranges are shown as one standard deviation of the mean value.

We previously reported<sup>18</sup> that surface relaxations from static calculations of the KDP (101) surfaces under nitrogen conditions compare closely (in direction and magnitude) to the experimental results of Reedjik.<sup>30</sup> Unfortunately, there are no experimental results for (101) surfaces under high vacuum conditions, as the surface quality was found to change over time, making it impossible to accurately determine the surface relaxations.<sup>7</sup> Comparing the surface relaxations in Table 3, both static and MD calculations predict an outward displacement of the  $\text{K}^+$  and  $\text{H}_2\text{PO}_4^-$  layers, matching the experimental trends, although there is some variation in the magnitudes of these relaxations. The calculated surface relaxations for the hydrated surfaces are larger than the experimental values, with the static 0 K results actually closer to those from experiments. As mentioned before, DFT calculations are known to overestimate the strength of hydrogen bonds. Examining the hydrated surfaces, we find that a number of strong hydrogen bonds with typical values of 1.4–1.7 Å have formed between the  $\text{H}_2\text{PO}_4^-$  layer and the neighboring water molecules. There is also an attraction between the  $\text{K}^+$  ions and the water molecules. These interactions could account for the larger surface relaxations observed in our static and MD calculations.

The position of the water atoms above the (101) surface gives insight into the nature of the interactions of water with the surface. Experimental surface XRD studies by Reedjik et al.<sup>8</sup> suggest that there are two well-ordered “ice-like” layers closest to the surface, then several quasi-ordered layers adjacent to these layers. The two well-ordered layers are predicted to have strong interactions with the (101) surface species. The oxygen atom positions in the first ordered water layer are predicted to be at the extrapolated position of a next potassium layer. Reedjik et al.<sup>8</sup>

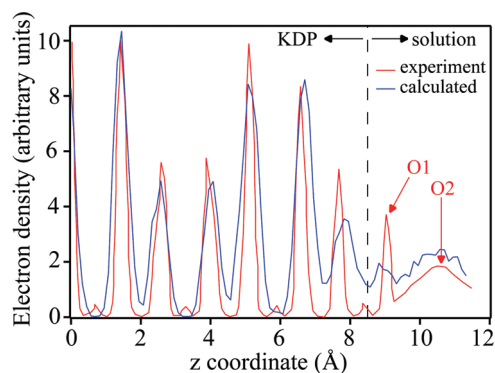


**Figure 4.** Electron density normal to the (101) surface from MD calculations of hydrated surfaces and experimental values extracted from Figure 8 of Vlieg et al.<sup>13</sup> O1 and O2 refer to the positions of the first and second ordered water layers from experimental studies of Vlieg et al.<sup>13</sup>.

report that the first ordered oxygen layer is approximately 1.3 Å above the surface  $\text{K}^+$  layer. Using the molecular dynamics results, we extracted the “z” coordinates of the water oxygen atoms and the potassium atoms to compare to the experimental values. As noted above, we find strong hydrogen bonds, typically 1.4–1.7 Å, between the layer of water molecules closest to the surface and the  $\text{H}_2\text{PO}_4^-$  ions.

A convenient way to visualize the molecular dynamics results of the hydrated surface is by projecting the electron density normal to the (101) surface. In Figure 4, we plot the electron density normal to the (101) surface for the hydrated MD surface and compared this to the experimental results extracted from Figure 8 of Vlieg et al.<sup>13</sup> In Figure 4, the sharp peaks at approximately 0, 1.3, 5.1, and 6.4 Å correspond to layers containing P atoms in  $\text{H}_2\text{PO}_4^-$ , and the sharp peaks at approximately 2.7, 4.0, and 7.8 Å correspond to  $\text{K}^+$  layers (with 7.8 being the outermost layer). Experimental SXR results<sup>13</sup> show a sharp oxygen peak at approximately 9.1 Å, corresponding to the first ordered water layer located approximately 1.3 Å above the surface  $\text{K}^+$  layer, labeled O1 in Figure 4. Experimental results also show a second quasi-ordered (and much broader) water layer peak, labeled O2 in Figure 4, a similar distance farther out from the first ordered water. Our MD results in Figure 4 show a small peak corresponding to the first ordered water layer at approximately the same location as found experimentally. The MD results in Figure 4 also show a similar broad peak for the quasi-ordered second water layer, matching well with experimental findings.

Using the translational and lateral displacements of the ice-like O1 layer, it is possible to calculate the mean squared deviation for this layer. A comprehensive molecular dynamics study of hexagonal ice by Tanaka and Mohanty<sup>31</sup> reports that the mean square deviation in the quantum harmonic approximation varies from 0.06 to 0.12 Å<sup>2</sup> for temperatures ranging from 150 to 250 K. The calculated mean square displacement for the ice-like O1 layer studied here is approximately 0.06 Å<sup>2</sup> in both the translational and lateral directions. Given the limited time frame accessible to this study (10 ps), compared to the classical molecular dynamics calculations of hexagonal ice, which uses a minimum of 15 ns of simulation time, the calculated mean square displacement compares quite favorably with the classical molecular dynamics study, strongly suggesting the O1 layer on the (101) surface exhibits ice-like behavior.

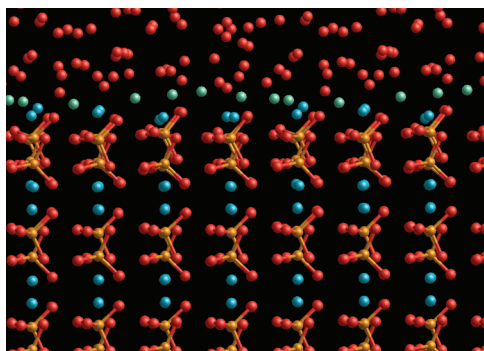


**Figure 5.** MD averaged hydrated surface of KDP. Hydrogen atoms have been removed for clarity. The green colored spheres represent oxygen atoms in water molecules that have two hydrogen bonds to the KDP surface and correspond to the 1st ordered water layer illustrated in Figure 4. Oxygen, potassium, and phosphorus atoms are represented by red, blue, and orange colored spheres, respectively.

To further illustrate the first ordered water on the KDP surface, in Figure 5, we show the MD averaged surface with water molecules highlighted (colored green), that form at least two hydrogen bonds to the KDP surface. The first ordered water layer indeed appears to correspond to water atoms that form multiple strong hydrogen bonds to the KDP surface. The location of this strongly bound water at the KDP surface in Figure 5 would thus correspond to the O1 peak in the Figure 4 density plot.

## CONCLUSIONS

We performed *ab initio* molecular dynamics calculations of the high- and low-temperature phases of bulk KDP. For the high temperature phase, we find evidence to support the theory that hydrogen atoms oscillate between two off-center positions in the high temperature phase. We have for the first time presented the results for *ab initio* molecular dynamics calculations on (101) surfaces of KDP. In general, we find good agreement with our previous study using static calculations,<sup>18</sup> and with the experimental results from SXRD studies, in particular with reference to the direction of the relaxation, although there is some variation in the magnitudes of the relations. We find a water layer that is strongly hydrogen bound to the KDP surface corresponding to a first ordered water layer, matching closely to experimental results. We also find a second quasi-ordered water region further out from the surface, also in agreement with experimental results. In the future, the next step would be to include the effect of ions in the solution of water to study the effect of pH on the surface relaxations. SXRD studies<sup>11,12</sup> show that the (100) surface is insensitive to pH, but the (101) surface is affected by the pH, so molecular dynamics simulations could provide insight into the interactions between the surface and the solvent.

## AUTHOR INFORMATION

### Corresponding Author

\*E-mail: a.rohl@curtin.edu.au.

## ACKNOWLEDGMENT

The authors thank iVEC and the NCI for the provision of computational resources.

## REFERENCES

- (1) Lin, Z.; Wang, Z.; Chen, C.; Lee, M. H. *J. Chem. Phys.* **2003**, *118*, 2349–2356.
- (2) Nelmes, R. J.; Tun, Z.; Kuhs, W. F. *Ferroelectrics* **1987**, *71*, 125–141.
- (3) Bastie, P.; Lajzerowicz, J.; Schneider, J. R. *J. Phys. C: Solid State Phys.* **1978**, *11*, 1203–1216.
- (4) Baur, W. H. *Acta Crystallogr., Sect. B* **1973**, *29*, 2726–2731.
- (5) Nelmes, R. J. *Ferroelectrics* **1987**, *71*, 87–123.
- (6) De Vries, S. A.; Goettkindt, P.; Bennett, S. L.; Huisman, W. J.; Zwanenburg, M. J.; Smilgies, D. M.; De Yoreo, J. J.; van Enckevort, W. J. P.; Bennema, P.; Vlieg, E. *Phys. Rev. Lett.* **1998**, *80*, 2229–2232.
- (7) De Vries, S. A.; Goettkindt, P.; Huisman, W. J.; Zwanenburg, M. J.; Feidenhans'l, R.; Bennett, S. L.; Smilgies, D. M.; Stierle, A.; De Yoreo, J. J.; Van Enckevort, W. J. P.; Bennema, P.; Vlieg, E. *J. Cryst. Growth* **1999**, *205*, 202–214.
- (8) Reedijk, M. F.; Arsic, J.; Hollander, F. F. A.; De Vries, S. A.; Vlieg, E. *Phys. Rev. Lett.* **2003**, *90*, 066103.
- (9) Odelius, M.; Bernasconi, M.; Parrinello, M. *Phys. Rev. Lett.* **1997**, *78*, 2855–2858.
- (10) Thiel, P. A.; Madey, T. E. *Surf. Sci. Rep.* **1987**, *7*, 211–385.
- (11) Kaminski, D.; Radenovic, N.; Deij, M. A.; Van Enckevort, W. J. P. *Phys. Rev. B* **2005**, *72*, 245404.
- (12) Kaminski, D.; Radenovic, N.; Deij, M. A.; Van Enckevort, W. J. P.; Vlieg, E. *Cryst. Growth Des.* **2006**, *6*, 588–591.
- (13) Vlieg, E.; Deij, M. A.; Kaminski, D.; Meekes, H.; Van Enckevort, W. J. P. *Faraday Discuss.* **2007**, *136*, 57–69.
- (14) Koval, S.; Kohanoff, J.; Migoni, R. L.; Bussmann-Holder, A. *Comput. Mater. Sci.* **2001**, *22*, 87–93.
- (15) Koval, S.; Kohanoff, J.; Migoni, R. L.; Tosatti, E. *Phys. Rev. Lett.* **2002**, *89*, 187602.
- (16) Zhang, Q.; Kioussis, N.; Demos, S. G.; Radousky, H. B. *J. Phys.: Condens. Matter* **2002**, *14*, L89–93.
- (17) Wang, K.; Fang, C.; Zhang, J.; Liu, C. S.; Boughton, R. I.; Wang, S.; Zhao, X. *Phys. Rev. B* **2005**, *72*, 184105.
- (18) Carter, D. J.; Rohl, A. L.; Gale, J. D. *J. Chem. Theory Comput.* **2006**, *2*, 797–800.
- (19) Stack, A. G.; Rustad, J. R.; De Yoreo, J. J.; Land, T. A.; Casey, W. H. *J. Phys. Chem. B* **2004**, *108*, 18284–18290.
- (20) Soler, J. M.; Artacho, E.; Gale, J. D.; Garcia, A.; Junquera, J.; Ordejon, P.; Sanchez-Portal, D. *J. Phys.: Condens. Matter* **2002**, *14*, 2745–2779.
- (21) Troullier, N.; Martins, J. L. *Phys. Rev. B* **1991**, *43*, 1993–2006.
- (22) Perdew, J. P.; Burke, K.; Ernzerhof, M. *Phys. Rev. Lett.* **1996**, *77*, 3865–3868.
- (23) Zhang, Q.; Chen, F.; Kioussis, N.; Demos, S. G.; Radousky, H. B. *Phys. Rev. B* **2001**, *65*, 024128.
- (24) Koch, W.; Holthausen, M. C. *A Chemist's Guide to Density Functional Theory*, 2nd ed.; Wiley-VCH Verlag GmbH: Weinheim, Germany, 2001.
- (25) Bacon, G. E.; Pease, R. S. *Proc. R. Soc. London, Ser. A* **1955**, *230*, 359–381.
- (26) Blinc, R. J. *Phys. Chem. Solids* **1960**, *13*, 204–211.
- (27) Reiter, G. F.; Mayers, J.; Platzman, P. *Phys. Rev. Lett.* **2002**, *89*, 135501.
- (28) Liu, C. S.; Kioussis, N.; Demos, S. G.; Radousky, H. B. *Phys. Rev. Lett.* **2003**, *91*, 015505.
- (29) Ogorodnikov, I. N.; Pustovarov, V. A.; Shul'gin, B. V.; Kuanyshev, V. T.; Satybaldieva, M. K. *Opt. Spectrosc.* **2001**, *91*, 224–231.
- (30) Reedijk, M. F. *Ordering at solid-liquid interfaces*. PhD Thesis, University of Nijmegen, The Netherlands, 2003.
- (31) Tanaka, H.; Mohanty, U. *J. Am. Chem. Soc.* **2002**, *124*, 8085–8089.